Electromagnetic Field Correlation inside a Sonoluminescing Bubble

Pritiraj Mohanty
Condensed Matter Physics 114-36, California Institute of Technology, Pasadena, CA 91125
(February 6, 2008)

We consider the correlation of the electromagnetic field to determine spatial coherence inside a sonoluminescing bubble. We explicitly calculate the first order correlation function for two limiting cases of the excitation field: a blackbody spectrum and a discrete multifrequency spectrum. The correlation length for blackbody fields at temperatures between 3000 K and 10000 K is found to be on the order of the optical wavelength, increasing with decreasing temperatures. We predict spectral lines in the emission spectrum of single bubble sonoluminescence in cooler bubbles with interior temperatures below 10000 K.

PACS numbers: 78.60.Mq, 42.50Fx, 34.80.Dp, 03.65.Bz

Sonoluminescence is the outburst of a short light pulse from a noble gas bubble acoustically levitated in a liquid by ultrasound [1,2]. Some of its salient features are the short duration of outburst with a pulsewidth—typically on the order of picoseconds [3–5], the large number of photons per outburst—typically on the order of a million, and the wide emission spectrum over and probably beyond the visible range. Recently, it has been argued that cooperative decay of excited states of metastable molecules could explain the light emission so peculiar in SL [6–8].

The theory of collective decay or lasing [6,7] of the population-inverted medium of molecules naturally contains the short timescale of the sonoluminescence pulse and the large number of photons emitted per outburst. In single bubble sonoluminescence, the emitted spectrum, however, is found to be a continuum, often devoid of any structure resembling the spectral lines of the gas molecules of either the solute or the solvent. It is natural then to assume, though naively, that the emission mechanism is not compatible with a lasing process which is expected to be monochromatic. This argument is not correct for the reason that cooperative emission does indeed occur for a collection of molecules with a broad distribution of wavelengths. The input driving field which establishes this polychromatic distribution can be correlated over a length comparable to the relevant scale in sonoluminescence. This scale defines the length over which molecules are correlated through the common electromagnetic field. It also determines the number of correlated molecules N_{eff} and hence the number of emitted photons. A large N_{eff} is essential in the proposed mechanism [6,7] as it determines the coherent part of the decay, $I_{coherent} \propto N_{eff}^2$; the incoherent part of the emission goes as N, the total number of emitting entities.

In this paper we address this specific question pertaining to the excitation of the gas molecules necessary for population inversion. Considering that the gas in the sonoluminescing bubbles can reach a temperature of 10000 K ($\sim$ 1 eV), or even higher [9,10], it is important to determine if there is correlation in the electric field at these temperatures. Towards that end, we calculate the first order correlation function for a generalized excitation field in two limits of high ($k_BT \gg \hbar\omega$) and low ($k_BT \ll \hbar\omega$) interior temperature where the excitation is dominated by (a) a blackbody field and (b) a discrete multifrequency field arising from atomic/molecular lines, respectively. For the blackbody field, we find that the first-order correlation length in the electric field is on the order of the wavelength in the visible range, which allows the collection of excited molecules to be correlated over this length scale. With increasing temperature this correlation length is found to decrease substantially. Discrete multiple frequency fields corresponding to the spectral lines are also found to have long correlation lengths. We find that the correlation in the excitation is dominated by a blackbody field in hottor bubbles whereas discrete multiple frequency fields dominate at temperatures below 10000 K.

We predict that the spectral lines will be observable in single bubble sonoluminescence (SBSL) at temperatures below 10000 K; these discrete lines are expected to be prominent in the blue part of the emission spectrum. The discrete lines were not observed in the SBSL spectrum in previous experiments because of extremely high temperatures inside the bubbles. This explains the experimental observation [11] that the sodium D-lines are visible in multiple bubble sonoluminescence (MBSL), which are now known to be at a typical gas temperature of 5000 K [12]; the D-lines were absent in the SBSL spectrum because the single bubbles were much hotter. Our analysis allows us to understand, for the first time, the connection between multiple bubble sonoluminescence [12,13] and single bubble sonoluminescence, namely they occur due to the same mechanism though in different temperature regimes.

Coherence in an atom-field system is best understood by studying the electromagnetic field modes [14–16]. If N excited atoms distributed over a range of frequencies decay coherently, the photon number in the correspond-

ing modes of the number state of the electromagnetic field coupled to the atoms will change accordingly. Since the atoms and the field form a closed system, it is then equivalent and even useful to consider coherence in the field modes.

The degree of coherence is often expressed by the cross correlation $\langle E(\mathbf{r}_1,t_1)E(\mathbf{r}_2,t_2)\rangle$ and higher order correlations $\langle E(\mathbf{r}_1,t_1)E(\mathbf{r}_2,t_2).....\rangle$ in the field variable $E(\mathbf{r},t)$. For example, the first order correlation is relevant for double-slit type interference experiments. The intensity is governed by the superposition of the amplitude contributions: $E_Q(t_2-t_1) = c_1E(\mathbf{r}_1,t_1) + c_2E(\mathbf{r}_2,t_2)$. This results in an additional part $2Re\langle c_1E(\mathbf{r}_1,t_1)c_2E(\mathbf{r}_2,t_2)\rangle$ to the intensity $|E_Q(t_2-t_1)|^2$ coming from first order interference. This interference term is a complex function in general and it describes the first order coherence (two-point correlation function in the field). Similarly, higher order coherences are defined by the higher order correlation functions. For example, four-point correlation function defines the second order coherence relevant for the Hanbury-Brown and Twiss experiment. Our calculation of higher order coherence which signifies purely quantum mechanical effects will be presented elsewhere.

The first order coherence function is defined by

$$C(\mathbf{r}_1,\mathbf{r}_2;t_1,t_2) \equiv \langle E_i(\mathbf{r}_1,t_1)E_j(\mathbf{r}_2,t_2)\rangle, \tag{1}$$

where $\langle\ldots\rangle$ denotes the ensemble averaging through a density matrix opertaor ρ such that $\langle E_iE_j\rangle = Tr[\rho E_iE_j]$, and $\rho = (1/Z)exp(-\beta H)$. The definition of ρ is physically important, and may include the active medium transitions. A multifrequency electric field can be expanded in terms of the monochromatic fields $E_i(\mathbf{r},t) = \sum_\omega E_{i\omega}(\mathbf{r},t)$. If the temperature inside the bubble is very high, then the dominant contribution to the correlation function will come from the blackbody field, and hence, ρ could be determined for a known temperature T. At intermediate temperatures, the active medium becomes important and the spectral contribution from the transitions in the given system must be taken into account as well. In both cases ρ factorizes into operators for each frequency ω and $\rho = \Pi_\omega\rho_\omega$. Each ω component of the field may be assumed to be independent of each other, in which case the number state representation of the field reduces to product of the number states of individual frequencies, i.e. $|n_{\omega_1}n_{\omega_2}\ldots\rangle = \Pi_{\omega_i}|n_{\omega_i}\rangle$. Then the correlation function has the following expression:

$$\langle E_i(\mathbf{r}_1,t_1)E_j(\mathbf{r}_2,t_2)\rangle = \sum_\omega\sum_{n_\omega}\langle n_\omega|E_{i\omega}(\mathbf{r}_1,t_1)E_{j\omega}(\mathbf{r}_2,t_2)|n_\omega\rangle\langle n_\omega|\rho_\omega|n_\omega\rangle. \tag{2}$$

The product of fields at two points may be given as

$$E_i(\mathbf{r}_1,t_1)E_j(\mathbf{r}_2,t_2) = \sum_\omega \frac{\omega^2}{c^2}(a_\omega a_\omega^\dagger e^{-i\omega(t_1-t_2)}A_{i\omega}(\mathbf{r}_1)A_{i\omega}^\dagger(\mathbf{r}_2) + h.c.), \tag{3}$$

which follows from the definition of $E(\mathbf{r},t) = \frac{i}{c}\sum_\omega\omega(a_\omega exp[-i\omega t]A_\omega(r) + h.c.)$ assuming Coulomb gauge in the interaction picture. The diagonal terms in a_ω and $a_\omega^\dagger$ such as $a_\omega a_\omega$ are ignored in the following.

The quantization for each mode ω requires that $a_\omega a_\omega^\dagger + a_\omega^\dagger a_\omega = \frac{\hbar}{2\omega}[2n_\omega+1]$. Ignoring the second term, which represents vacuum fluctuations, one obtains an expression for the symmetrized correlation function:

$$Tr[\rho(E_iE_j + E_jE_i)/2] = [\sum_{n_\omega=0}^{\infty} exp[-\frac{n_\omega\hbar\omega}{kT}]]^{-1}\sum_\omega\sum_{n_\omega}\frac{\hbar\omega}{c^2}n_\omega exp[-\frac{n_\omega\hbar\omega}{kT}]Re(exp[-i\omega(t_i-t_j)]A_{i\omega}(\mathbf{r}_1)A_{j\omega}^*(\mathbf{r}_2)). \tag{4}$$

In the above equation, for equal times, the summation over the occupation number n_ω yields the usual Planck's law. We consider the effect of active medium via a distribution function:

$$f(\omega) = g_{\omega_p}\delta(\omega-\omega_p), \tag{5}$$

where the strengths of different lines are given by g_{ω_p} and ω_c is a cutoff frequency. This function will depend on the composition of the gas (solute) inside the bubble and the surrounding liquid (solvent). The effect of temperature and pressure inside the bubble can be taken into account by replacing the δ-function by a Lorentzian with a full width at half maximum corresponding to inhomogeneous broadening. $f(w,p)$ may also be a continuous function in case of an ionic spectrum which are realized in very hot bubbles. The final spectrum of emitted light would contain both $f(\omega,p)$ and the Planck spectrum. At high temperatures, the Planck distribution would dominate over the emission line distribution. For the emission lines to be observable in SBSL, the temperature inside the bubble must satisfy the condition

$$g_{\omega_p}\hbar\omega_p \gg \frac{\hbar\omega_p}{e^{\hbar\omega_p/k_BT}-1}. \tag{6}$$

At high temperatures, the right hand side of the inequality becomes equal to k_BT. In order to see the lines in the emission spectrum of SBSL at a wavelength λ, the interior temperature has to be reduced below $T^* = hc/\lambda k_B$. The visible range of 200 nm $\rightarrow$ 700 nm in wavelength corresponds to a temperature range of 71000 K $\rightarrow$ 20000 K.

Eq. 4 gives the complete expression of correlation of fields in any arbitrary shape. For $r_i = r_j$ and $t_i = t_j$, it

reduces to the Planck distribution. The vector potential $\mathbf{A}(r)$ satisfies the Helmholtz equation:

$$\nabla^2 \mathbf{A}_\omega + \omega^2 \epsilon(r) \mathbf{A}_\omega = 0, \tag{7}$$

with appropriate boundary conditions. For a gas bubble with an average dielectric constant ϵ_1 immersed in a liquid with a dielectric constant ϵ_2. The solution of the Helmholtz equation is normally constructed from the linear combination of the solutions of the scalar field equation, requiring that $\mathbf{E}_\perp$, ϵE_r, B_r and $\mathbf{B}_\perp/\mu$ be continuous across the bubble surface, i.e. at $r = a$. With the use of the boundary conditions, the transverse electric (TE) and transverse magnetic (TM) mode solutions $(A_r, A_\theta, A_\phi)^{TE,TM}$ can be constructed inside and outside the bubble [17,18].

I. Blackbody field: Analytic evaluation of the coherence function with the exact solutions of Eq. (7) is rather complicated. Here we give results for the limiting case of wavelengths short compared to the minimum bubble radius, $r \gg \lambda$. However, in standard SBSL experiments the minimum bubble radius is usually on the order of the wavelength. Even though $r \simeq \lambda$, closed-form expressions are possible only in this case. This condition is strictly satisfied in the case of millimeter-sized laser-induced bubbles [19].

Let us choose a direction for the wave vector k as $(\sin\theta\cos\phi, \sin\theta\sin\phi, \cos\theta)$. The coherence function in the longitudinal [20] direction is given by

$$C_1^{long}(r,t) \simeq \frac{1}{r^2}\int_0^\infty [g_{\omega_p}\delta(\omega-\omega_p)\hbar\omega + \frac{\hbar\omega}{e^{\hbar\omega/k_BT}-1}]\hbar\omega d\omega[\frac{\sin kr}{kr} - \cos kr]\cos\omega\tau. \tag{8}$$

where $\omega = kc$. If the thermal contribution dominates, $T \gg \hbar\omega/k_B$, then the spectral distribution is essentially Planckian. This high temperature result was first obtained by Bourret [21] who derived the second-order electric correlation tensor of blackbody radiation using techniques similar to those employed in the theory of isotropic turbulence of an incompressible fluid. The high temperature limit of the above result [22] reduces to

$$C_1^{long}(r,0) \sim \frac{1}{r^2}\int_0^\infty \frac{kdk}{e^{\alpha k}-1}(\frac{\sin kr}{kr} - \cos kr) \propto \frac{1}{r^3}(1 - r\frac{\partial}{\partial r})\frac{1}{\alpha}L(\frac{r}{\alpha}) \tag{9}$$

where, $\alpha = c\tau_\beta$, and $\tau_\beta = \hbar/k_BT$ is the thermal time. $L(x) = \pi/2\coth\pi x - 1/2x$ is the standard Langevin function. The expression in Eq. 9 is plotted in Fig. 1 for three different temperatures of the blackbody field. The scale over which correlation reduces to a characteristic value, the coherence length R_ϕ, is seen to vary between 0.5 to 0.2 μm for bubble temperatures ranging from 3000 K to 10000 K. This mesoscopic scale of coherence length is

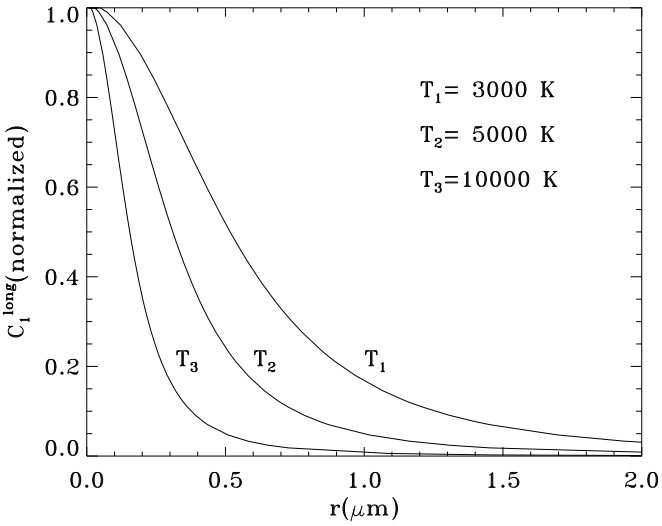

FIG.1 Variation of the normalized coherence function at three different temperatures.

comparable to the compressed bubble size. At temperatures above 20000 K, the correlation length is found to be less than 0.1 μm.

II. Discrete field: At low enough temperatures $g\hbar\omega_p \gg k_\beta T$, coherence in the field of a set of discrete emission lines can be studied in a similar manner [23]. The coherence function C_1^{long} in the long wavelength limit becomes equal to

$$C_1^{long}(k_p, r, 0) \sim g_{\omega_p} k_p^3 [\frac{1}{3} - \frac{(k_p r)^2}{30} + O((k_p r)^4)]. \tag{10}$$

The r dependence of C_1^{long} is parabolic, and a coherence length R_ϕ can be defined as the scale over which C_1^{long} is reduced to a characteristic value, half of its maximum. For a given wavelength λ_p,

$$R_\phi \sim \lambda_p/\pi. \tag{11}$$

In the lowest order, coherence is seen to be strongly dependent on the wavelength ($\lambda_p = 2\pi/k_p$),

$$C_1^{long} \sim \lambda_p^{-3}. \tag{12}$$

Hence SL from the discrete spectral lines in the blue part of the spectrum should be stronger than that in the red part. This is true for the coherent radiation in the SL emission spectrum. Observation of such a trend is a strong indication that the emitted light is indeed partly coherent.

In the blackbody regime, the correlation length is much less than 0.05 μm at a typical temperature of 40000 K; thus the effective number of molecules participating in collective decay reduces greatly as $N_{eff} = \rho(4\pi R_\phi^3/3)$, where ρ is the average density. The sonoluminescence

emission spectrum is not dominated by coherent emission. $I_{incoherent} \sim N \propto R_{min}^3$, and $I_{coherent} \sim N_{eff}^2 \propto R_\phi^6$. For a typical minimum bubble radius R_{min} of 0.5 μm and a total N of 10^6, the incoherent emission is comparable to the coherent emission. At higher temperatures, incoherent emission dominates.

Another corroborating evidence towards the transition from high temperature to low temperature behavior can be obtained from the temporal shape of the emitted light pulse. The pulse shape should progressively change from either $sech^2$ or oscillatory behavior (signifying ringing) [7] to exponential decay which signifies incoherent emission [9,10,24].

Let us summarize the three important aspects of the emission spectrum following our analysis: (a) Bubbles with an interior temperature much above 70000 K will typically display a blackbody emission spectrum in the entire visible range. As the temperature is reduced, spectral structure will appear in the blue part of the emission spectrum, progressing towards the red part. Experimentally, it is found that the spectrum is blackbody and almost identical at long wavelengths, while it is gas specific at short wavelengths [4], consistent with our picture. Below 10000 K, the emission spectrum will show atomic/molecular lines in the entire visible range. (b) The lines in the spectrum would be less strong in the red part as the correlation length for a discrete field decreases with increasing wavelength very sharply: $C_1^{long} \sim \lambda^{-3}$. (c) Our analysis provides a natural connection between SBSL and MBSL surrounding the question as to why spectral lines are conspicuously absent in conventional SBSL experiments, but distinctly present in MBSL [11,12]. This is primarily because the gas temperature in MBSL is on the order of 5000 K, whereas in SBSL it's much higher.

In conclusion, we show that the electromagnetic field inside a sonoluminescing bubble has a finite correlation even at high temperatures. At high temperatures ($T \gg$ 40000 K) the emission spectrum is expected to be predominantly blackbody. At low temperatures ($T <$ 10000 K) discrete emission lines are predicted in single bubble sonoluminescence. Our analysis explains the parametric differences between multibubble sonoluminescence and single bubble sonoluminescence, exemplified by their very different emission spectra.

I thank Prof. Lawrence Crum whose questions motivated this work. I am also grateful to Prof. Gary Williams, Ohan Baghdasarian, and Prof. Woowon Kang for helpful conversations.

[1] D.F. Gaitan, L.A. Crum, R.A. Roy, and C.C. Church, J. Acoust. Soc. Am **91**, 3166 (1992).
[2] For some recent reviews see B. P. Barber *et al.* Phys. Rep. **281**, 65 (1997); L. A. Crum *et al.*, Science **266**, 233 (1994); L. A. Crum, Phys. Today **47** (September), 22 (1994).
[3] B. Gompf *et al.*, Phys. Rev. Lett. **79**, 1405 (1997).
[4] R. Hiller, S. Putterman, S. Weninger, Phys. Rev. Lett. **80**, 1090 (1998).
[5] M. J. Moran *et al.*, Nuc. Ins. Phys. Res. B **96**, 651 (1995); M.J. Moran, and D. Sweider, Phys. Rev. Lett. **80**, 4987 (1998)
[6] P. Mohanty, S.V. Khare, Phys. Rev. Lett. **80**, 189 (1998).
[7] P. Mohanty, cond-mat/9912271.
[8] A.M. Brodsky, Mod. Phys. Lett. **13**, 1019 (1999).
[9] W.C. Moss, D.B. Clarke, D.A. Young, Science **276**, 1398 (1997); Phys. Rev. E **59**, 2986 (1999).
[10] S. Hilgenfeldt, S. Grossmann,D. Lohse, Nature **398** 402 (1999); Physics of Fluids **11**, 1318 (1999).
[11] T. Matula *et al.*, Phys. Rev. Lett. **75**, 2602 (1995).
[12] W.B. McNamara, Y.T. Didenko, and K.S. Suslick, Nature **401**, 772 (1999).
[13] A. Giri, and V.H. Arakeri, Phys. Rev E **58**, R2713 (1998).
[14] R. Glauber, Phys. Rev. **130**, 2529; **131**,2766 (1963).
[15] C. L. Mehta, J. Math. Phys. **8**, 1798 (1967).
[16] M. Born, and E. Wolf, *Principles of Optics* (Pergamon Press, Inc., New York, 1959).
[17] K.A. Milton, and Y.J. Ng, Phys. Rev. E **55**, 4207 (1997).
[18] C. Eberlein, Phys. Rev. A **53**, 2772 (1996).
[19] O. Baghdassarian, B. Tabbert, and G.A. Williams, Phys. Rev. Lett. **83**, 2437 (1999).
[20] This corresponds to the coherence of the fields along the z-axis if z-axis is chosen to be along **r**.
[21] R.C. Bourret, Nuovo Cimento **18**, 347 (1960).
[22] C.L. Mehta, and E. Wolf, Phys. Rev. **134**, A1143 (1964); *ibid.* A1149 (1964).
[23] H.M. Nussenzveig, J. Math. Phys. **8**, 561 (1967).
[24] L. Frommhold, A.A. Atchley, Phys. Rev. Lett. **73**, 2883 (1994); L. Frommhold, Phys. Rev. E **58**, 1899 (1998).